A COMMERCIAL MEV-UED INSTRUMENT BASED ON A 2.5 CELL RF-PHOTOGUN*

J. Kraemer, V. Kuemper†, C. Quitmann, A. Ufer, RI Research Instruments GmbH, Bergisch Gladbach, Germany
M. Pfeiffer, RWTH Aachen University, Aachen, Germany

Abstract

Research in quantum, nano, and energy materials requires atomic-scale information in space and time. Such materials exhibit ultrafast phenomena such as light absorption, structural changes, phase transitions, and thermal or non-thermal melting on ps to sub-ps timescales with Ångström-scale motion. We present the conceptual design of the RI-Bornite MeV-UED instrument, based on a copper 2.5-cell RF photogun with a replaceable Cu photocathode. A single Ti:Sa fs laser drives both the pump beam (266 nm, ca. 1 µJ/pulse) and the probe beam (800 nm, few mJ/pulse). The system is designed to achieve 100 fs temporal resolution. The current sample chamber is optimized for solid samples and supports sample cooling and a load-lock; future versions will enable liquid and gas experiments. We present the design considerations, electron beam dynamics simulations, and engineering design.

INTRODUCTION

MeV ultrafast electron diffraction (MeV-UED) is a powerful technique for studying atomic-scale processes in materials science, chemistry, biology, physics, and related fields [1]. It reveals ultrafast (fs) phenomena such as phase transitions, light absorption, and structural changes.

We present the conceptual design of the first commercial MeV-UED system.

A MODULAR ROBUST INSTRUMENT

We aim for a robust design reliably achieving sub 100 fs temporal resolution and allowing future upgrades. It builds on proven instruments [1, 2, 3]. The electron beam is created in a 2.5 cell RF-electron gun by a UV laser pulse (50 fs, 266 nm). It is focused using a single solenoid and an aperture allows cutting out the off-axis beams. The sample chamber is designed for solid samples and includes the beam path for the IR pump laser and mechanical stages for sample positioning. Two detectors are in the far-field with an adjustable distance up to 5 m. We consider a hybrid pixel detector and a scintillation detector based on an electron-multiplied CCD camera.

The instrument includes the RF-klystron and low-level RF (LLRF) system as well as the fs laser system and an EPICS based control system. This allows controlling the e-beam, the laser beam, the sample and acquiring the data. Data analysis can be done by one of the many open-source codes for diffraction.

The configuration and parameters described in Figure 1 and Table 1 are the design goals for a basic instrument. Optional upgrades include:

- Gaseous or liquid samples
- Optical Parametric Amplifier (OPA)
- Electron pulse compression
- Solenoids for focussing the e-beam at the sample or the detector
- Two separate lasers for pump and probe with delays up to µs and dedicated synchronization

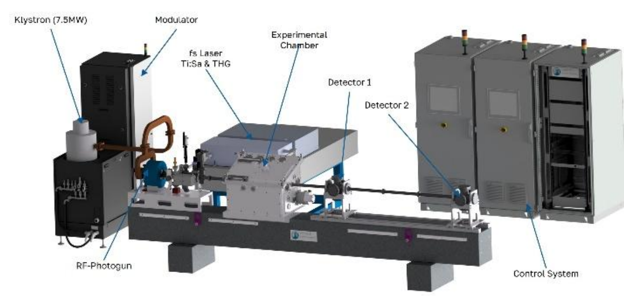

Figure 1: CAD model of the MeV-UED instrument.

Figure 2 shows a schematic overview. A part of the Ti:Sa laser beam is used as the probe beam (THG → 266 nm) generating the electrons from a Cu-photocathode. The pump beam is guided via a motorized delay line, enters the sample chamber and is directed onto the sample via a mirror.

The sample stage is adjustable in x / y, R_x / R_y.

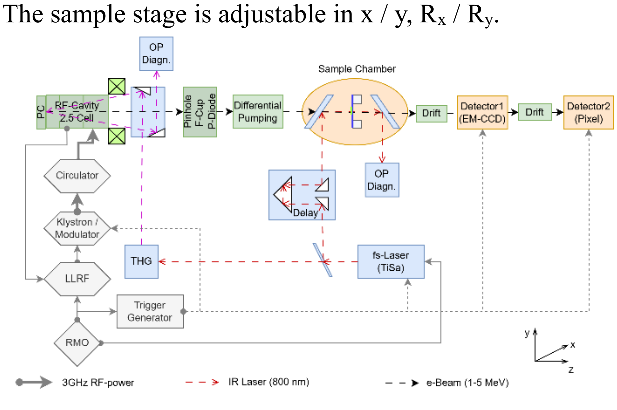

Figure 2: Schematic overview of the MeV-UED System.

The main contribution to time resolution is the electron bunch length at the sample. It is estimated to $\Delta t_{probe,rms} \approx$ 66 fs. The RF will deliver stabilities of $\sigma_{E,amp,rms} \approx$ 0.05 MV/m in amplitude and $\sigma_{E,phase,rms} \approx 0.1°$ in phase. Simulations indicate a timing mismatch between pump and probe of $\Delta t_{amp,rms} = 30$ fs and $\Delta t_{phase,rms} = 30$ fs from these RF jitters. The pump laser pulse has a pulse width of $\Delta t_{pump\ pulse,rms} = 15$ fs. Additionally, the pump laser has an arrival jitter which is estimated to $\Delta t_{pump\ jitter,rms} =$ 30 fs. This all adds up to:

$$\Delta t_{total,rms} = \left(\Delta t_{probe}^2 + \Delta t_{amp}^2 + \Delta t_{phase}^2 + \Delta t_{pump\ pulse}^2 + \Delta t_{pump\ jitter}^2\right)^{\frac{1}{2}} = \text{ca.}\,85\ \text{fs}$$

With second order effects, vibration and temperature instabilities we anticipate a total time resolution of $\Delta t_{tot} \leq$ 100 fs.

Table 1: Design goal of a basic instrument

Parameter	Design Goal
Time Resolution:	100 fs
Electron Energy	3 - 7 MeV (optimized for 5 MeV)
Rep. Rate	Up to 1000 Hz possible
Bunch Charge	~ 60 fC (ca. 4 10^5 electrons) for best t-resolution ~ 3 pC (ca. 2 10^7 electrons) for single-shot experiments
Detectors	~ 1M Pixels, 75µm pixel size, <2 kHz read out rate Scintillator screen read out by EM-CCD (1M pixel, 13 µm, <50 fps)
Spot diameter @ sample	ca. 160 µm (rms)
Laser energy per pulse	< 5 mJ/pulse
Laser energy range	800 nm (Ti:Sa)
Delay range	1 ns, 10 fs/step
Sample environment	Room temperature solid sample mounted on motorized stages
Momentum resolution	ca. <0.05 Å^{-1}
Delivery time	ca. 20 months
Software	Experiment control and data acquisition included. Data analysis not included.

2.5 CELL RF-PHOTOGUN

The electron gun uses a 2.5 cell S-band design (Figure 3) based on brazed copper parts. Compared to designs with fewer cells, the 2.5-cell design has lower power density, enabling higher energy and thus shorter bunches with improved long-term stability [3]. The photocathode is a copper stub, which can be replaced after venting the gun. The 1st full cell includes a pick-up for RF-field measurement and LLRF control. The second cell is connected to a symmetric RF coupler, where two RF and two pump ports symmetrize the RF field. The gun is fed by the klystron (up to 7.5 MW, 1.5 µs pulse length). It allows maximum fields of 120 MV/m at the PC. To avoid excessive dark currents the design foresees operation at ca. 80 MV/m under normal conditions. PC-laser in-coupling occurs from the front via adjustable all-metal mirrors inside the UHV, enabling near-normal incidence and a round spot.

The gun is currently in fabrication and will be tested in 2027.

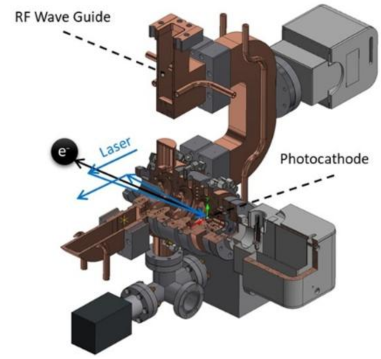

Figure 3: 2.5 cell RF-gun.

ELECTRON BEAM DYNAMICS

We used ASTRA [4] and GPT [5] to investigate the electron beam dynamics and optimize emittance and temporal resolution. To benchmark our simulations, we compare this 2.5 cell gun with the 1.6 cell gun operated successfully at SLAC [2]. Figure 4 shows the RMS-spot size of the electron beam vs. beam propagation (z) for three different electron energies.

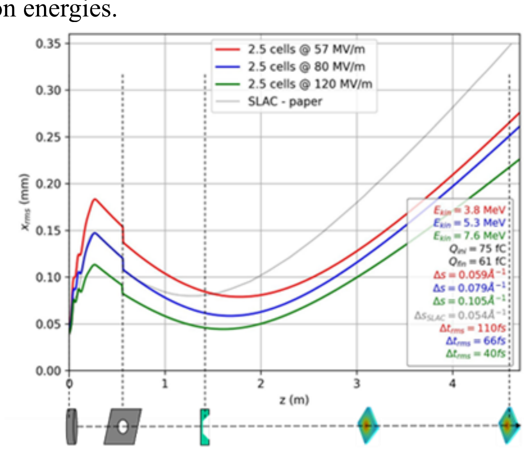

Figure 4: Electron beam diameter vs. distance to photocathode for various field strength of the 2.5 cell gun in comparison to the SLAC [4] gun (grey line).

After the PC the spot size grows due to the Coulomb repulsion. The solenoid (z ~ 0.4 m) focusses the beam onto the sample position. The aperture (z ~ 0.57 m) only slightly clips the main beam but massively attenuates dark current and off-axis beams. The sample is located near the e-beam focus (z ~ 1.16 m). Here the e-beam spot size is between ca. 50 – 100 µm depending on the electron energy. High fields at the PC lead to rapid acceleration to relativistic energies and thus reduce the Coulomb repulsion resulting in smaller spot sizes on the sample. The electron energy can be varied between ca 3.8 and 7.6 MeV. The higher the energy, the thicker a sample can be penetrated.

Figure 5 shows the emittance ε_n vs. beam propagation. After the PC the emittance decreases because of the acceleration in the RF-field, at the aperture it is reduced by ca. 20% by clipping off-energy and high-angle electrons, see Figure 6, middle row (z = 0.57 m). Phase space plots of the electrons are shown in Figure 6.

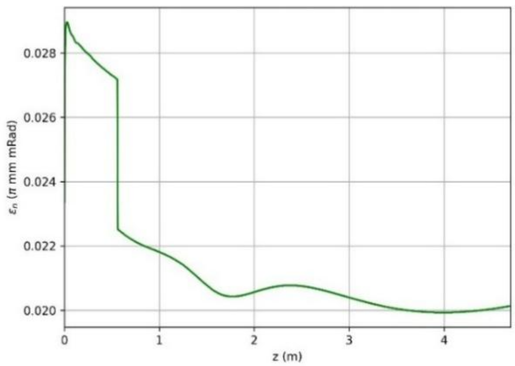

Figure 5: Normalized transverse emittance along the e-beam.

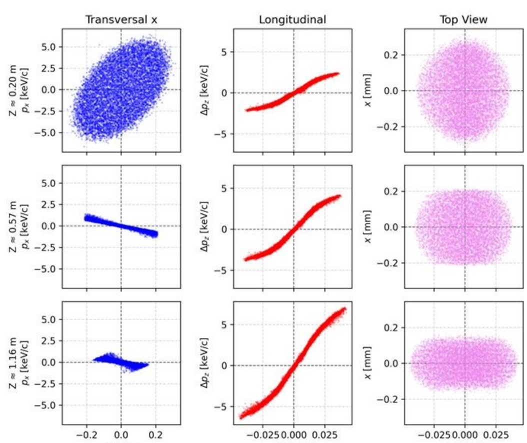

Figure 6: Phase space of the electrons at three positions (z = 0.2 m immediately after the gun, z = 0.57 m position of pinhole, and z = 1.16 m sample position).

SAMPLE CHAMBER

The sample chamber shown in Figure 7 is designed for solid samples and allows installation of relatively bulky custom equipment placed on bread boards. Access during installation is provided through a large lid on the top, allowing two people to work inside the chamber. Spare flanges allow installing additional pumps, feedthroughs, etc. Samples mounted on the standard flag style sample holder can be introduced via a load-lock. This load lock contains a storage rack holding five sample plates with several samples per plate. The samples can be mounted on SiN membranes, graphene, 3 mm TEM grids, etc.

The laser is fed into the chamber from the back side where a long-distance microscope also allows *in-situ* sample observation. Additional ports allow user adaptation for sample cooling, electrical contacts and other features. Inside the chamber the sample can be positioned into the electron focus and can be rotated around the x- and y-axis to meet the Bragg diffraction condition.

For the laser beam the focus and overlap with the electron beam is detected using a fluorescent screen mounted on a sample plate and the long-distance microscope.

The sample chamber can be adapted to specific requirements.

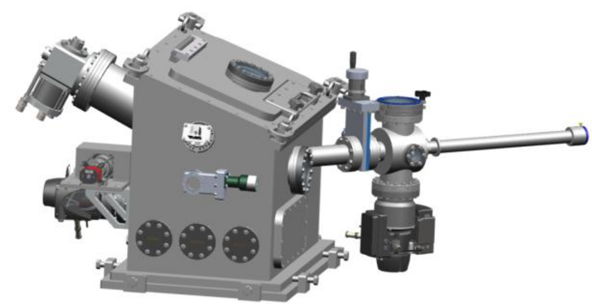

Figure 7: Sample chamber seen along the e-beam path showing load lock (right), large lid for access (top), cryo-cooler (top left) and long-distance microscope (bottom left).

CONCLUSION

We demonstrate the suitability of a 2.5 cell RF gun for MeV-UED. This provides a narrow (x_{rms} < 100 µm), low emittance (ε_n = ca. 0.2 π mm mRad) beam with variable energy of ca. 3.5 – 7.5 MeV and sub 100 fs temporal resolution.

Providing the instrument as a fully commercial device installed and tested at the customer site will open the technique of MeV-UED to users who have so far not been able to conduct such experiments on their most interesting sample due to limited availability of such a system.

ACKNOWLEDGEMENT

The authors thank Xijie Wang (University of Dortmund) and S. Eisebitt (Max Born Institute Berlin) for helpful discussions.

REFERENCES

[1] D. Filippetto, et al. "Ultrafast electron diffraction: Visualizing dynamic states of matter.", Reviews of modern physics 94.4, 045004 (2022).

[2] S. P. Weathersby, et al. "Mega-electron-volt ultrafast electron diffraction at SLAC National Accelerator Laboratory", Rev. Sci. Instrum. 86, 73702 (2015).

[3] B. L. Militsyn, et al. "High repetition rate highly stable s-band photocathode gun for the clara project", IPAC 2013: Proceedings of the 4th International Particle Accelerator Conference. 437-439 (2013).

[4] A Space Charge Tracking Algorithm, Klaus Floettmann / © DESY (1997), see: https://www.desy.de/~mpyflo/

[5] General Particle Tracer (GPT), S.B. van der Geer and M.J. de Loos, see: https://www.pulsar.nl/gpt/.